energies

MDPI

Article

Assessment of Fuel Cells' State of Health by Low-Frequency Noise Measurements

Arkadiusz Szewczyk [1,*], Łukasz Gaweł [2], Kazimierz Darowicki [2] and Janusz Smulko [1]

[1] Department of Metrology and Optoelectronics, Gdańsk University of Technology, ul. G. Narutowicza 11/12, 80-233 Gdańsk, Poland; janusz.smulko@pg.edu.pl
[2] Department of Electrochemistry, Corrosion and Materials Engineering, Gdańsk University of Technology, ul. G. Narutowicza 11/12, 80-233 Gdańsk, Poland; lukasz.gawel@pg.edu.pl (Ł.G.); kazdarow@pg.edu.pl (K.D.)
* Correspondence: szewczyk@eti.pg.edu.pl

Abstract: We proposed applying low-frequency (flicker) noise in proton-exchange membrane fuel cells under selected loads to assess their state of health. The measurement set-up comprised a precise data acquisition board and was able to record the DC voltage and its random component at the output. The set-up estimated the voltage noise power spectral density at frequencies up to a few hundred mHz. We observed the evolution of the electrical parameters of selected cells of different qualities. We confirmed that flicker noise intensity varied the most (more than 10 times) and preceded changes in the impedance or a drop in the output DC voltage (less than 2 times). The data were observed for current loads (from 0.5 to 32 A) far from the permissible load. We deduce that the method can be utilised in industrial conditions to monitor the state of health of the selected cells by noise analysis. The method can be used in real-time when the flicker noise is measured within the range of a few Hz and requires a reasonable amount of averaging time to estimate its power spectral density. The presented method of flicker noise measurement has considerable potential for use in innovative ways of fuel cell quality monitoring.

Keywords: electrochemical noise; flicker noise; fuel cell; state of health; reliability

Citation: Szewczyk, A.; Gaweł, Ł.; Darowicki, K.; Smulko, J. Assessment of Fuel Cells' State of Health by Low-Frequency Noise Measurements. *Energies* **2021**, *14*, 8340. https://doi.org/10.3390/en14248340

Academic Editor: Nicu Bizon

Received: 7 November 2021
Accepted: 8 December 2021
Published: 10 December 2021

1. Introduction

The green energy revolution requires reliable and inexpensive energy sources. This issue has attracted numerous researchers and encouraged governments to financially support such technological development. Fuel cells are a promising candidate for such an energy source, converting the fuel's energy of chemical bonding into electrical energy without greenhouse gas emissions. The cells utilise hydrogen to generate electrical power without polluting the environment [1]. The electrical energy produced can meet the demands of customers with various needs at all times. Proton-exchange membrane fuel cell (PEMFC) technology meets such requirements. This technology enables modular construction with easier sealing than competing designs, and rapid start-up even at low operating temperatures [2,3]. Unfortunately, this technology still needs enhancement due to numerous parameters affecting its reliability and durability [1,2].

The technology of fuel cells has recently seen several advancements [2]. Mostly, new materials and progress in fuel cell design have improved their use. However, this energy source's harsh internal working conditions accelerate numerous deterioration mechanisms [4,5]. Consequently, accurate diagnostics of faults such as dry-out, cell flooding, limited transport of reagents, disturbance of proton diffusion through the membrane, contaminants, starvation, and carbon corrosion in the PEMFC are critical to prolonging the proper operation of fuel cells. A few factors (e.g., overheating, undesirable electrochemical reaction [6]) that require monitoring to protect the cell against accelerated workout should be enumerated. Fuel cells work in a stack, and the failure of any single cell has a detrimental

impact on the whole pile by inducing even total breakdown [7]. This issue is fundamental when we consider the expected development of power grids into a network of renewable energy sources of various characteristics, requiring continuous adaptation and varying loads. Fuel cells can buffer other energy sources by multiple switching on and off of their loads and are therefore exposed to accelerated deterioration.

Flicker noise levels can assess the quality and reliability of electronic components and structures [8,9]. The corrosion rate or its type is detectable by electrochemical noise [10–16]. Batteries [17,18], supercapacitors [19], and fuel cells (FCs) [20–25] have also been investigated by utilising this phenomenon. Electrochemical energy sources are susceptible to any, even fragile, transitions in the electrode–electrolyte interface. Flicker noise (1/f noise) should potentially be very efficient in assessing the state of health of any changes within this interface because these changes can generate redundant, low-frequency fluctuations. This means that the evolution of noise intensity should manifest any tiny modifications in the state of health of fuel cells. We assume that noise should be more sensitive to such shifts than other electrochemical parameters (e.g., impedance, the temperature resulting from the working conditions).

Furthermore, low-frequency noise is characterised by the level and dependence of the power spectral density on the frequency, which can be particularly useful for the identification of the state of health of the tested fuel cells [24,25]. Some experiments proved this conclusion for their early degradation stage [25]. Unfortunately, low-frequency noise requires a sensitive measurement set-up [26] and additional data processing as in the case of other electrochemical noise data [27,28]. Moreover, electrochemical processes are slow or very slow, often within the frequencies of a few mHz only. Therefore, electrochemical noise requires a long recording time to estimate their statistical parameters with an acceptable level of random error. Such processes can even be non-stationary and involve more complicated methods of analysis.

The experimental studies proposed in this manuscript are focussed on the issues of noise measurements in a working fuel cell stack to monitor fuel cell state of health in industrial conditions. The applied set-up required some severe practical problems to be solved because low-level voltage signals must be recorded in the presence of intense loading currents and the switching control unit, which induce severe interferences. A noise-measurement methodology and a simplified method of noise analysis to assess the state of health of the investigated cells are proposed, and are a novelty of the applied approach. Our approach differs from the reported data, which consider experimental studies in laboratory conditions only [24,25].

Fuel cells were prepared in the same way and set up in a single stack, but they were of different quality due to the increasingly harsh working conditions as the stack deepened, which induced some unavoidable differences due to technological tolerance. Most of the published works present results of noise measurements in a single proton exchange membrane with the required alimentation and control equipment only. We observed fluctuations in the load current or potential of the fuel cells for defined conditions (e.g., temperature, humidity, pressure of the supplied gases, and loading resistances). The presented studies consider a stack of fuel cells working under various loads. By using simultaneous measurements, it is possible to compare the noise generated concurrently in individual cells and under similar operating conditions. Thus, the condition of the entire fuel cell stack is monitored by observing the states of the individual cells. This helps to predict the eventual stack failure. Our experimental studies imply that noise is more receptive to any slight changes within the cells than other electrical parameters, such as impedance, or generated DC voltage. This conclusion is crucial for preventing accelerated wear-out of FCs (e.g., induced by overheating). Real-time monitoring of the intensity of flicker noise signals any disturbances in the FCs at an early stage as compared to the other considered methods reporting on the state of wear.

The paper is organised as follows: the applied measurement set-up is presented in detail in Section 2; the studies of the noise measurements are discussed in Section 3, and

the conclusions are given in Section 4 to highlight the utility of the practical application of noise measurements for the state-of-health monitoring of fuel cells.

2. Measurement Set-Up

The PEMFC stack was supplied by Zentrum für Sonnenenergie-und Wasserstoff Forschung Baden-Württemberg ZSW (Ulm, Germany) [29]. It consisted of ten individual cells with an active, geometrical surface area of 96 cm^2 each. A commercially available membrane electrode assembly with 0.5 mg/cm^2 platinum loading was used. Flow channels based on a cascaded flow field design with parallel-connected multiple serpentine groups were located in bipolar plates. We switched the tested device about 10,000 times between the loading currents of 5 A and 130 A.

A test stand controlled the stack operation (Fuel Cell Technologies Inc., Albuquerque, NM, USA). An electronic load (Keysight Co., SantaRosa, FL, USA) was used. The experimental studies were executed under the enumerated working circumstances:

- stack temperature: 75 °C;
- air and hydrogen backpressure: 150 kPa (abs);
- relative humidity of air and hydrogen: 50%;
- flow rate of hydrogen: 5 $dm^3 \cdot min^{-1}$ (99.999% purity);
- flow rate of air: 15 $dm^3 \cdot min^{-1}$.

Electrochemical impedance spectroscopy (EIS) was applied to pre-assess the state of health. EIS is a commonly known and approved method to assess the state of health of FCs [30,31]. The EIS was measured using a PXIe 6164 and a PXIe 4497 board (National Instruments, USA Company, Austin, TX, USA) to generate a multi-sinusoidal excitation signal and to acquire the response. An excitation had a sufficient amplitude of 5% of the DC load. The signal was the sum of 21 harmonics of frequencies between 0.3 Hz and 2.84 kHz with the optimised amplitudes and phase shifts of each harmonic to limit the resulting amplitude—the excitation signal—which was composed as presented. The lowest frequency excitation signal limited the measurement time for each spectrum.

We observed voltage fluctuations between the terminals of the anode and cathode for each selected cell. The control unit automatically switched the selected loading currents (0.5 A, 1 A, 2 A, 4 A, 8 A, 16 A, and 32 A). This induced electromagnetic interference, which was present in the recorded voltage fluctuations between the electrodes of the selected cells. A data acquisition card recorded voltage signals with a 24-bit analogue-to-digital (A/D) converter (National Instruments, model NI-USB-4431). A block diagram showing the measurement setup is presented in Figure 1. The diagram comprises a control unit and a voltage acquisition board attached directly to the cell electrodes. The card has four independent voltage inputs and a build-in anti-aliasing filter—the applied A/D converter allowed voltage fluctuations between the cell electrodes to be observed without additional amplification. We configured the inputs of the data acquisition device for differential measurement with DC coupling. The sampling frequency was set to f_S = 1024 Hz, and the set-up recorded 500 records of 4096 samples each for the selected load current. The observation time for each load was about 33 min. Some of the noise records from the set of 500 were rejected because of visible interference, but at least 200 records were used to evaluate each power spectral density (PSD). The number of averaged spectra assured a random error of the estimated PSD below 8% ($1/200^{0.5} \approx 0.0707$ [26]), which is acceptable for noise measurements. We applied the simplest method of avoiding spike-like interference by rejecting some of the time series. This prolonged the time of measurements to obtain an acceptable level of random error. We should mention that other methods can be applied in practical applications (e.g., saturation of the noise amplitude at the selected level during the presence of a spike). Such a process reduces the measurement time and should have a limited impact on the accuracy of the estimated noise power spectral density. This modification can be used in practice after being thoroughly tested and approved for industrial applications.

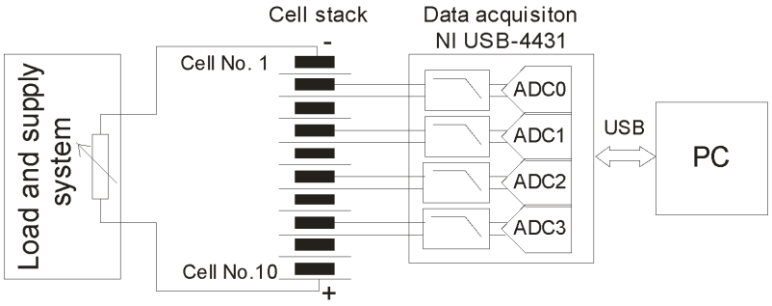

Figure 1. Schematic diagram of the applied test stand.

Four cells (No. 2, 4, 6, and 8) were selected to record voltages between the electrodes of the cells by using all of the available measurement channels. The recorded voltage time series comprises DC (direct current) voltage, noise component, and interference. A slow harmonic part of a frequency lower than 2 mHz and short, intense spike interference induced by switching off the stack control unit were observed during switching on and off a water distribution system and pump relays.

The cells were numbered starting from No. 1 at the anode side of the stack. We opted to investigate two various sets of the cells in-depth: two sections with a high state of health (No. 2, 4) manifested by high output voltages, and two sections (No. 6, 8) exhibiting lower output voltage and therefore having a diminished state of health.

3. Experimental Results and Discussion

3.1. Impedance Spectra Measurements

Figure 2 shows the impedance spectra for cells No. 2 and No. 4 at the selected loading currents. Each measured impedance spectrum has the shape of a flattened semi-circle. The impedances decreased with an increase in the loading current, as expected for healthy cells in the considered range of currents. Cell No. 4 was still operating in the ohmic overpotential region in comparison to cell No. 2, in which we observed a concentration polarisation region for the highest loading current. This behaviour is related to the limited diffusion of oxygen into the catalyst layer [30–32].

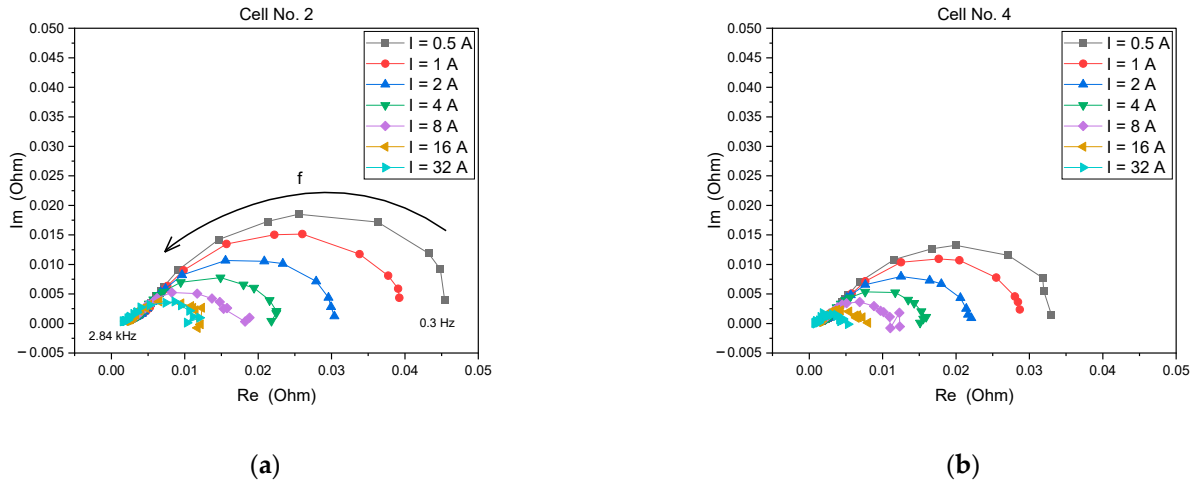

(**a**) (**b**)

Figure 2. Impedance spectra of the power cells for different current loads I: (**a**) cell No. 2, (**b**) cell No. 4; the impedance (real Re and imaginary Im parts) measurements were recorded at frequencies from 0.3 Hz to 2.84 kHz.

Figure 3 shows impedance spectra for the cells with lower states of health (No. 6 and No. 8) than the samples reported earlier (No. 2 and No. 4) at the same loading currents. The impedance of cell No. 6 (Figure 3a) changes abnormally when compared to the results reported for the other tested cells at increasing loading currents. Moreover, some results

show that the sample was non-stable during the measurements (e.g., at the loading current I = 16 A—Figure 3a). These results indicate damage to this cell. The damage of this cell suggests problems with gas transport to the catalyst. This can be caused by poor water management or ageing of the gas diffusion layer (GDL).

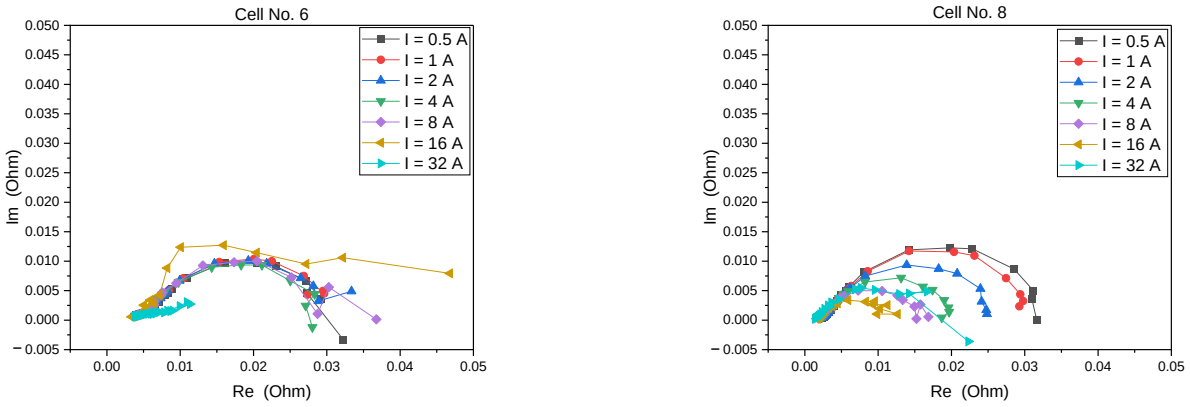

(**a**) (**b**)

Figure 3. Impedance spectra of the power cells for different current loads I: (**a**) cell No. 6, (**b**) cell No. 8; the impedance (real Re and imaginary Im parts) measurements were recorded at frequencies from 0.3 Hz to 2.84 kHz.

The impedance spectra recorded for cell No. 8 (Figure 3b) are similar to those recorded for cells No. 2 and No. 4. We observed an increase of impedance for the highest loading current I = 32 A. This suggests, analogously to the healthy cells No. 2 and No. 4, that cell No. 8 was in a region of mass transfer losses for this loading current.

Based on the presented impedance data, we can conclude that cell No. 4 is operating correctly. Cell No. 6 is practically fully damaged, and cells No. 2 and No. 8 are of an intermediate state of health—they are working correctly for low loading currents and show some minor symptoms of dysfunctionality at higher loading currents.

3.2. Low-Frequency Noise Measurements

The recorded voltage time series were subjected to DC component removal by subtracting the estimated mean value. In the next step, the PSD of a random component was calculated by the fast Fourier transform (FFT) algorithm and averaging (Welch method).

The voltage records contain interference originating from the stack control system. To avoid the influence of such components on the noise analysis results (high-frequency components in the estimated PSD), the time series with those components (short voltage pulses) were rejected from the analysis. Figure 4 shows typical time courses of the voltage of a cell for a 4 A load with the intense pulses caused by a water distribution system and/or pump relays. As can be seen, the pulses are identically distributed for different cells. We rejected those parts of the signal from further analysis. Each record of 4096 samples was checked for the presence of pulses whose amplitudes were too high by performing a thresholding operation before the FFT calculation. If short pulses were present, the record was rejected. The threshold level was selected arbitrarily for each time series and equalled the standard deviation σ multiplied by a factor of four. We excluded any time series exhibiting spikes of absolute value greater than 4σ from further processing and PSD estimation. This operation was not challenging, but we can propose more efficient variants without excluding the recorded time series from data processing and restraining the measurement time necessary for noise analysis.

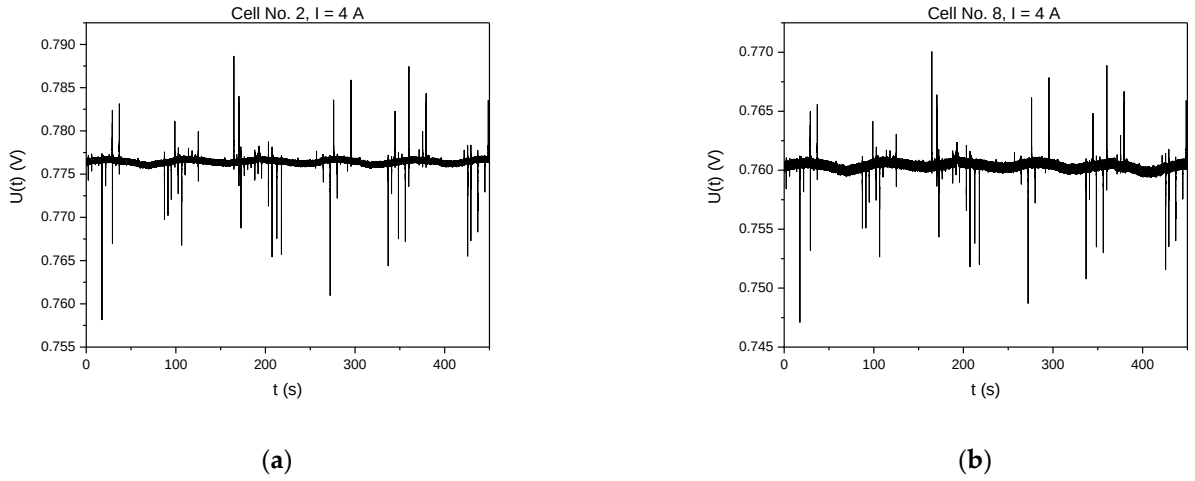

(**a**) (**b**)

Figure 4. Voltage time series U(t) observed between the cell's electrodes at a loading current of 4 A: (**a**) cell No. 2, (**b**) cell No. 8.

The DC values of the voltages across the cell were estimated for each recorded time series. Figure 5 shows the DC voltages versus loading currents for the investigated cells. It can be concluded that the voltages dropped similarly for cells No. 2, 4, and 8 when the loading current increased. Cell No. 6 showed the most flawed behaviour. The initial voltage, at the lowest loading current of 0.5 A, was about two times lower than for the other studied cells. At the loading current of 16 A, the voltage reached about 0 V, and at 32 A, it was negative. Therefore, low voltage between the terminals of cell No. 6 at its load indicates that this cell is of the most inferior quality within the set of studied cells. The negative voltage at the highest applied load current, which is still far from the maximum permissible nominal value for this fuel cell stack, is probably caused by damage to the membrane electrode assembly (MEA) inducing a decrease in the state of health of cell No. 6. It should be noted that the DC voltages of cells No. 8 and 2 are somewhat less intense than the values for No. 4. The apparent difference is rather subtle and cannot be related to eventual deterioration within the investigated cells.

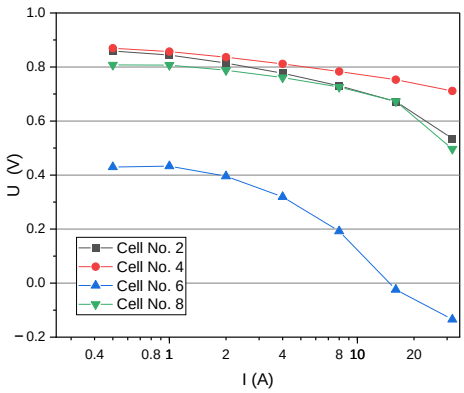

Figure 5. DC voltages U of the studied cells for selected loading currents I.

The estimated PSDs of the voltage noise component show a $1/f^{\alpha}$ dependence with the slope $\alpha \approx 2.5$ at frequencies below 10 Hz (e.g., Figure 6a,b). Such a shape is typical for FCs, as reported elsewhere [23]. We observed a similar profile for all studied FCs (Figure 6). The main difference between two healthy cells (No. 2 and No. 4) was observed at the highest loading current I = 32 A. Cell No. 2 had about a two times more intense PSD at the mentioned current than the PSD of cell No. 4. At the same time, lower DC voltages were observed for cell No. 2 than for No. 4 (Figure 5), but the differences were of lower intensities than for noise.

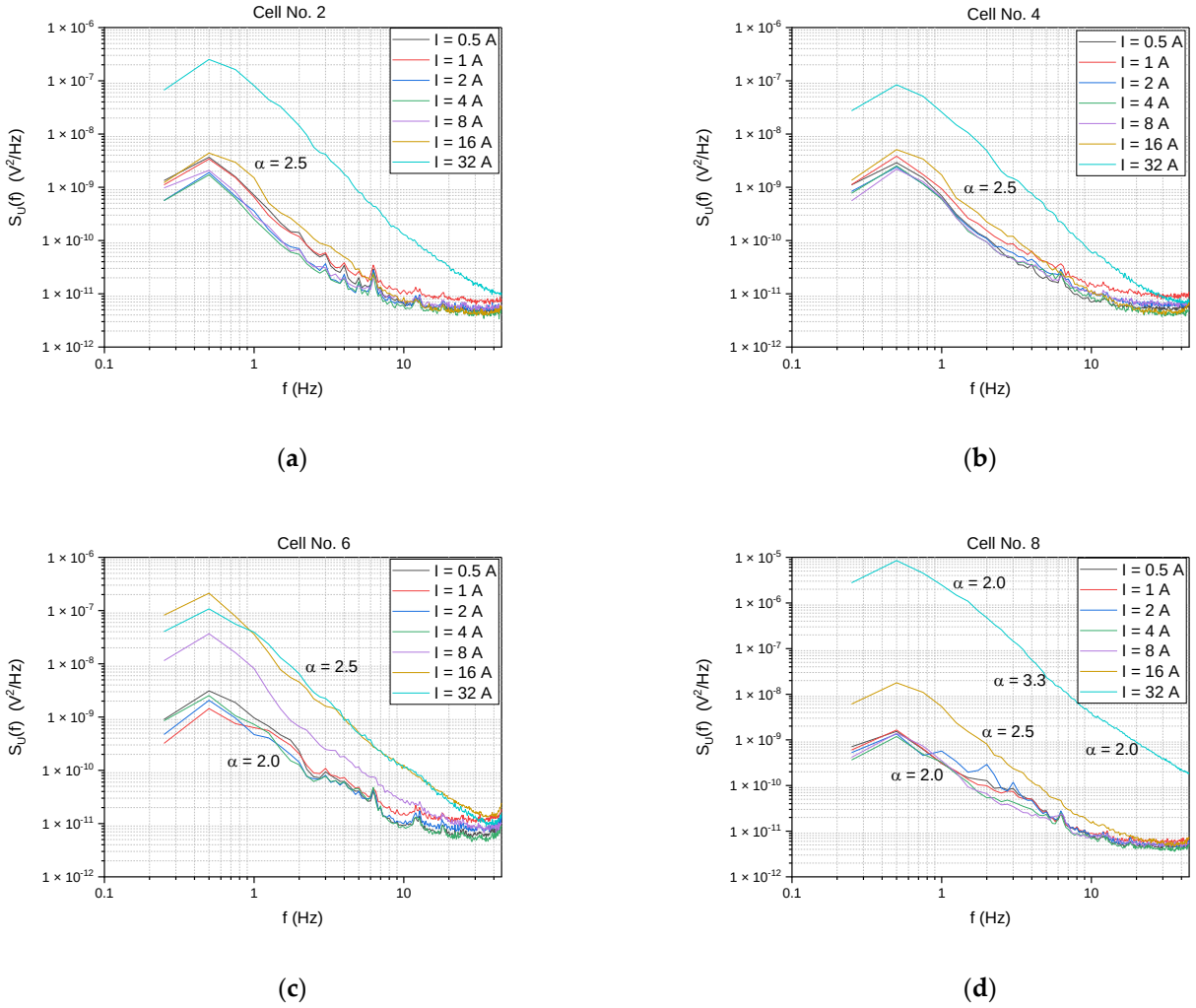

Figure 6. Power spectral density $S_u(f)$ of voltage fluctuations observed between the terminals of the cell versus frequency f for different loading currents I: (**a**) cell No. 2, (**b**) cell No. 4, (**c**) cell No. 6, (**d**) cell No. 8.

When we compare the results of the noise PSD measurements for cells No. 2 and No. 4 (Figure 6a,b) with the EIS results for both cells (Figure 2) we see that cell No. 2, having higher impedance (Figure 2a), exhibits a more intense PSD than cell No. 4 (about three times more intense—Figure 6a,b) at the highest loading current only. The slopes of the PSD spectra do not change. In addition, based on the impedance results, we can state that the increase in the PSDs in both cells is related to the mass transfer limitations.

Individual differences between cells No. 2 and No. 4 are also visible by a lower drop of the DC voltage observed when the loading current I increased for cell No. 4 (Figure 5), and are related to the lower impedance of this cell (Figure 2b). The impedances decreased with an increase in the loading current, as is expected for healthy cells in the considered range of currents. These results correspond with the voltage drop measurements and differences between both considered cells (Figure 5).

Figure 6c,d present the detailed noise PSDs for cells No. 6 and 8, respectively. The slope of the PSDs was lower ($\alpha \approx 2.0$) for these cells at the loading currents below a few amperes. It can be supposed that the mechanisms of noise generation under these conditions for cells No. 6 and 8 are different from the mechanisms responsible for noise generation for cells No. 2 and 4. Moreover, the same cells (No. 6 and 8) exhibited a faster increase in the estimated PSD under the same increase in loading currents than for cells No. 2 and 4 (Figure 6a,b). The most intense flicker noise was observed in cell No. 8 at the loading current I = 32 A. The PSD for cell No. 8 (Figure 6d) was up to two orders

of magnitude more intense than for cells No. 2 and 4 (Figure 6a,b). This suggests that low-frequency noise is susceptible to any changes within the cells' structures. Moreover, for cell No. 8, for the loading current I = 16 A, the slope α increased to 2.5. For the highest loading current I = 32 A, the slope α varies in the consecutive frequency ranges: below 1.25 Hz, α = 2.0; from 1.25 Hz to 10 Hz, α = 3.3; and above 10 Hz, α = 2.0 (Figure 6d). PSDs with different slopes are also reported in [22]. This phenomenon was related to incorrect water balance within the PEMFC structure and was observed at higher loading currents only [23].

The flicker noise observed in cell No. 6 began to increase at lower loading currents than in cell No. 8. Moreover, the DC voltage between its terminals was significantly lower and decreased much faster than in the case of cell No. 8 (Figure 5). Thus, cell No. 6 could be assessed as the most depleted cell within the batch of studied samples. This conclusion suggests that the intensity of the observed flicker noise is not the only factor that can be used to determine the state of health of the studied cell. We know that the statistics of electrochemical noise (e.g., amplitude probability distribution [12]) can determine corrosion type and can be manifested by changes in the slope of noise PSDs.

It is difficult to unambiguously explain the primary process which determines the intensity of the flicker noise made in the cell. Numerous experiments should be carried out while controlling changes in the cells' operating parameters to create a map of estimated noise PSDs depending on the relative humidity, operating temperature, loading current, mass flow, etc. These issues require intense future works. In a simplified approach, it can be considered that noise is a general predictor of the state of health of power cells. This approach is essential from a practical point of view because low-frequency noise can be monitored within the selected frequency range and can provide decisive information about the power cells. Moreover, the operation of flicker noise measurements at a fixed frequency bandwidth, and estimation of the averaged PSD at this bandwidth, can be performed by low-cost and commonly available electronic devices.

Similar results for PEMFCs have been reported elsewhere [23] and were related to incorrect water management in the fuel cells. They observed the same local changes in PSD slopes and a less intense increase in the estimated PSDs. The reported experiment [23] controlled the working conditions of the studied PEMFC by selecting the relative humidity of the supplied hydrogen and air for its work at given current densities. The mentioned results showed less intense noise changes than in the presented case because they investigated the same cell but at different levels of controlled humidity. In the studied stack and cells, it is not only the various features of water management that can vary. Primarily, any modifications in the resistance of the cell can affect the intensity of the low-frequency noise. Thus, noise measurements can be even more efficient for the evaluation of the state of health of the power cells than in the mentioned literature [23].

Figure 7 gathers noise data for all of the studied cells versus the loading current I (noise PSDs at the selected frequency of 1 Hz, where low-frequency noise prevails). The noise in cells No. 6 and No. 8 was more intense than in cells No. 2 and No. 4 at loading currents over I = 16 A. This effect started at even lower loading currents but was not as high for cell No. 8. The differences are quite huge and can reach even two orders of magnitude of the estimated PSDs. This result means that the relative changes in noise intensities are much more significant than the changes in DC voltage. It implies that noise data have potential for the early detection of deterioration processes within power cells even if the measurements are performed during their exploitation. The same conclusions were found to be true when the noise power spectral densities were selected for a higher frequency (3 Hz) but still in the range where low-frequency noise dominates.

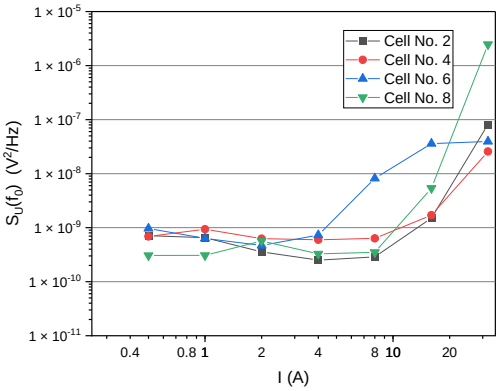

Figure 7. Power spectral density $S_u(f_0)$ of voltage fluctuations recorded between the terminals of the cell at the given frequency f_0 = 1 Hz versus loading current I.

It is worth emphasising that the recorded power spectral densities of noise are far above the inherent noise of the measurement set-up at the low-frequency range, which is typically 55 μV_{RMS} in the 20 kHz frequency range. Moreover, its intensity changed in a different way for the same loading currents for other power cells. These facts confirm that the observed noise was generated by processes taking place within the power cells.

We can simplify the presented method of noise measurements to estimate the mean square value of the voltage fluctuations within the selected bandwidth, as proposed in another application of flicker noise measurements by a simplified set-up based on a low-cost microcontroller [33]. The simplified measurements can also determine the slope of the low-frequency noise by selecting only two or three bands and evaluating a quotient of the estimated mean square values. This simplified method should be sufficient to assess the slope of 1/f noise which can determine the reasons for the predicted failure of the monitored fuel cells. It requires an operation of voltage sampling, squaring, and averaging. A microcontroller can easily perform all of the enumerated functions with limited memory resources for averaging. The low-frequency range of the observed fluctuations makes this task easier because of the low sampling frequency. The presented, abridged method can use the suggested set-up to monitor fuel cells in their operational state.

4. Conclusions

We measured the low-frequency noise generated within the individual cells of a PEMFC stack at selected loading currents. The noise data were compared with the impedance spectra and the DC voltages between the terminals of the studied samples under the same operating conditions. In conclusion, we can assess the state of health of cells by comparing noise levels between the exemplars and their eventual increase. Evident diversity was observed between the cells when the loading current was above 8 A. The samples in a poor state of health or damaged were identified by low-frequency noise at frequencies below only a few Hz. The DC voltage and electrochemical impedance spectroscopy measurements proved the conclusions drawn from the noise measurements. This means that noise measurements can assess the state of health of the tested fuel cell within a minute or so.

PSD noise is more sensitive to any changes within the cell than DC voltage only. PSD of electrochemical noise ($S_u(f_0)$ at f_0 = 1 Hz) was different between the cells more than 10 times with a sufficiently large current (above 20 A—Figure 7). In contrast, a voltage between their terminals (Figure 5) or the real part (Re) of their impedance (Figures 2 and 3) changed less than 2 times. Moreover, we can evaluate the slope of the estimated noise PSDs to shed light on the deterioration mechanisms in the monitored fuel cells. It is worth mentioning that the noise was measured directly as voltage fluctuations between the electrodes with no additional external load or any voltage amplification, during regular operation of the fuel cell stack. This shows that such measurements can be utilised to assess the state of health of an individual cell by monitoring voltage fluctuations. A low-cost measurement set-up, based

on commonly used microcontrollers, can be used to perform the necessary data recording and processing without any additional equipment or any disturbance of the operation of the stack. This is possible due to the low frequency of sampling and the ease of mathematical computing to estimate the PSD in selected frequency bands.

Moreover, the high sensitivity of the generated noise to any disruptions in the state of health of fuel cells can be very protective to them. Any dangers (e.g., during eventual overheating) to their operation can be quickly identified and mitigated by adapting their operating conditions. The proposed approach for fuel cells is novel and has not been presented before to the best of our knowledge.

It is worth underlining that the selected loading currents are still far from the nominal currents for the investigated type of PEMFC stack, which are about 100–120 A. When the DC voltage changes were compared to the PSD changes between the terminals of the studied fuel cells, it was found that the PSD noise may change by even more than 10 times for low-quality cells whereas the DC voltage changes much less. This means that the flicker noise level can be utilised as a perceptive test of the state of health of the power cell stack when monitored under operating conditions.

We underline that the applied method of noise data processing, as presented in detail elsewhere [12,34], can be further developed by considering the mechanisms of flicker noise generation and the methods used for its analysis.

Author Contributions: Formal analysis, A.S. and K.D.; funding acquisition, K.D.; investigation, A.S. and Ł.G.; methodology, A.S. and Ł.G.; project administration, A.S.; visualisation, A.S.; writing—original draft, A.S. and Ł.G.; writing—review and editing, J.S. All authors have read and agreed to the published version of the manuscript.

Funding: This research received no external funding.

Data Availability Statement: The data presented in this study are available in mostwiedzy.pl at doi.org/10.34808/jeb9-3257, reference: "fuel-cell-noise-data,212090912212847-0".

Conflicts of Interest: The authors declare no conflict of interest.

References

1. Staffell, I.; Scamman, D.; Velazquez Abad, A.; Balcombe, P.; Dodds, P.E.; Ekins, P.; Shah, N.; Ward, K.R. The role of hydrogen and fuel cells in the global energy system. *Energy Environ. Sci.* **2019**, *12*, 463–491. [CrossRef]
2. Konno, N.; Mizuno, S.; Nakaji, H.; Ishikawa, Y. Development of Compact and High-Performance Fuel Cell Stack. *SAE Int. J. Altern. Powertrains* **2015**, *4*, 123–129. [CrossRef]
3. Jayakumar, A. An Assessment on Polymer Electrolyte Membrane Fuel Cell Stack Components. In *Applied Physical Chemistry with Multidisciplinary Approaches*, 1st ed.; Haghi, A.K., Balköse, D., Thomas, S., Eds.; Apple Academic Press: Boca Raton, FL, USA, 2018; pp. 23–49. [CrossRef]
4. Borup, R.; Meyers, J.; Pivovar, B.; Kim, Y.S.; Mukundan, R.; Garland, N.; Myers, D.; Wilson, M.; Garzon, F.; Wood, D.; et al. Scientific Aspects of Polymer Electrolyte Fuel Cell Durability and Degradation. *Chem. Rev.* **2007**, *107*, 3904–3951. [CrossRef]
5. Mitzel, J.; Gülzow, E.; Kabza, A.; Hunger, J.; Araya, S.S.; Piela, P.; Alecha, I.; Tsotridis, G. Identification of critical parameters for PEMFC stack performance characterization and control strategies for reliable and comparable stack benchmarking. *Int. J. Hydrogen Energy* **2016**, *41*, 21415–21426. [CrossRef]
6. Cao, T.-F.; Lin, H.; Chen, L.; He, Y.-L.; Tao, W.-Q. Numerical investigation of the coupled water and thermal management in PEM fuel cell. *Appl. Energy* **2013**, *112*, 1115–1125. [CrossRef]
7. Hinaje, M.; Nguyen, D.; Raël, S.; Davat, B.; Bonnet, C.; Lapicque, F. Impact of defective single cell on the operation of polymer electrolyte membrane fuel cell stack. *Int. J. Hydrogen Energy* **2009**, *34*, 6364–6370. [CrossRef]
8. Vandamme, L.K.J. Noise as a diagnostic tool for quality and reliability of electronic devices. *IEEE Trans. Electron Devices* **1994**, *41*, 2176–2187. [CrossRef]
9. Jones, B. Electrical noise as a reliability indicator in electronic devices and components. *IEE Proc.—Circuits Devices Syst.* **2002**, *149*, 13–22. [CrossRef]
10. Hladky, K.; Dawson, J.L. The measurement of corrosion using electrochemical 1/f noise. *Corros. Sci.* **1982**, *22*, 231–237. [CrossRef]
11. Cheng, W.; Luo, S.; Chen, Y. Use of EIS, Polarization and Electrochemical Noise Measurements to Monitor the Copper Corrosion in chloride media at different temperatures. *Int. J. Electrochem. Sci.* **2019**, 4254–4263. [CrossRef]
12. Smulko, J.; Darowicki, K.; Zieliński, A. Detection of random transients caused by pitting corrosion. *Electrochim. Acta* **2002**, *47*, 1297–1303. [CrossRef]

13. Grafov, B.M.; Dobrovolskii, Y.A.; Klyuev, A.; Ukshe, A.; Davydov, A.D.; Astafev, E.A. Median Chebyshev spectroscopy of electrochemical noise. *J. Solid State Electrochem.* **2017**, *21*, 915–918. [CrossRef]
14. Smulko, J.; Darowicki, K.; Wysocki, P. Digital measurement system for electrochemical noise. *Pol. J. Chem.* **1998**, *72*, 1237–1241.
15. Cottis, R.A. Interpretation of Electrochemical Noise Data. *Corrosion* **2001**, *57*, 265–285. [CrossRef]
16. Ma, C.; Wang, Z.; Behnamian, Y.; Gao, Z.; Wu, Z.; Qin, Z.; Xia, D.-H. Measuring atmospheric corrosion with electrochemical noise: A review of contemporary methods. *Measurement* **2019**, *138*, 54–79. [CrossRef]
17. Martinet, S.; Durand, R.; Ozil, P.; Leblanc, P.; Blanchard, P. Application of electrochemical noise analysis to the study of batteries: State-of-charge determination and overcharge detection. *J. Power Sources* **1999**, *83*, 93–99. [CrossRef]
18. Astafev, E.A. Measurements and Analysis of Electrochemical Noise of Li-Ion Battery. *Russ. J. Electrochem.* **2019**, *55*, 488–495. [CrossRef]
19. Szewczyk, A. Measurement of Noise in Supercapacitors. *Metrol. Meas. Syst.* **2017**, *24*, 645–652. [CrossRef]
20. Legros, B.; Thivel, P.-X.; Bultel, Y.; Nogueira, R. First results on PEMFC diagnosis by electrochemical noise. *Electrochem. Commun.* **2011**, *13*, 1514–1516. [CrossRef]
21. Denisov, E.S.; Evdokimov, Y.K.; Martemianov, S.; Thomas, A.; Adiutantov, N. Electrochemical Noise as a Diagnostic Tool for PEMFC. *Fuel Cells* **2016**, *17*, 225–237. [CrossRef]
22. Astafev, E.A.; Ukshe, A.E.; Manzhos, R.A.; Dobrovolsky, Y.A.; Lakeev, S.G.; Timashev, S.F. Flicker Noise Spectroscopy in the Analysis of Electrochemical Noise of Hydrogen-air PEM Fuel Cell During its Degradation. *Int. J. Electrochem. Sci.* **2017**, *12*, 1742–1754. [CrossRef]
23. Maizia, R.; Dib, A.; Thomas, A.; Martemianov, S. Proton exchange membrane fuel cell diagnosis by spectral characterization of the electrochemical noise. *J. Power Sources* **2017**, *342*, 553–561. [CrossRef]
24. Astafev, E.A. Electrochemical Noise Measurement of Polymer Membrane Fuel Cell under Load. *Russ. J. Electrochem.* **2018**, *54*, 554–560. [CrossRef]
25. Astafev, E.A.; Ukshe, A.; Gerasimova, E.V.; Dobrovolsky, Y.; Manzhos, R.A. Electrochemical noise of a hydrogen-air polymer electrolyte fuel cell operating at different loads. *J. Solid State Electrochem.* **2018**, *22*, 1839–1849. [CrossRef]
26. Bendat, J.S.; Piersol, A.G. *Random Data: Analysis and Measurement Procedures*, 4th ed.; John Wiley and Sons: Hoboken, NJ, USA, 2011.
27. Astafev, E.A. Comparing the Method and Hardware for Electrochemical Impedance with the Method of Measuring and Analyzing Electrochemical Noise. *Russ. J. Electrochem.* **2018**, *54*, 1022–1030. [CrossRef]
28. Monrrabal, G.; Huet, F.; Bautista, A. Electrochemical noise measurements on stainless steel using a gelled electrolyte. *Corros. Sci.* **2018**, *148*, 48–56. [CrossRef]
29. Janicka, E.; Mielniczek, M.; Gawel, L.; Darowicki, K. Optimization of the Relative Humidity of Reactant Gases in Hydrogen Fuel Cells Using Dynamic Impedance Measurements. *Energies* **2021**, *14*, 3038. [CrossRef]
30. Darowicki, K.; Janicka, E.; Mielniczek, M.; Zieliński, A.; Gaweł, L.; Mitzel, J.; Hunger, J. The influence of dynamic load changes on temporary impedance in hydrogen fuel cells, selection and validation of the electrical equivalent circuit. *Appl. Energy* **2019**, *251*, 113396. [CrossRef]
31. Darowicki, K.; Janicka, E.; Mielniczek, M.; Zielinski, A.; Gaweł, L.; Mitzel, J.; Hunger, J. Implementation of DEIS for reliable fault monitoring and detection in PEMFC single cells and stacks. *Electrochim. Acta* **2018**, *292*, 383–389. [CrossRef]
32. Yuan, X.Z.; Song, C.; Wang, H.; Zhang, J. *Electrochemical Impedance Spectroscopy in PEM Fuel Cells*; Springer: London, UK, 2010. [CrossRef]
33. Kotarski, M.M.; Smulko, J.M. Hazardous gases detection by fluctuation-enhanced gas sensing. *Fluct. Noise Lett.* **2010**, *9*, 359–371. [CrossRef]
34. Astafev, E.A. Wide-frequency band measurement and analysis of electrochemical noise of Li/MnO2 primary battery. *J. Solid State Electrochem.* **2019**, *23*, 1705–1713. [CrossRef]